Appendix for

Li et al., “Rtt105 functions as a chaperone for Replication Protein A to preserve genome stability”

Appendix Contents:

Appendix Figure S1-S9

Appendix Table S1-S2

Appendix Supplementary materials and methods

Appendix Figure S1

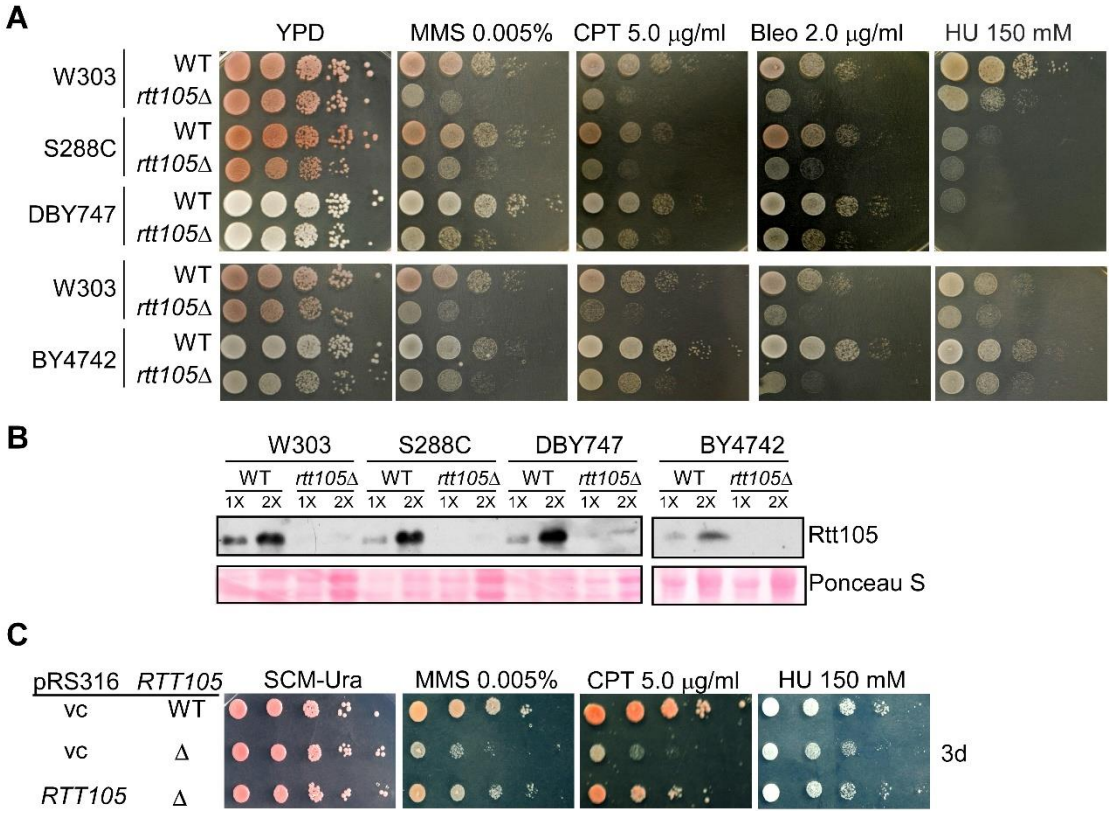

Fig S1. Deletion of *RTT105* caused increased DNA damage sensitivity to CPT, MMS, HU but not lethal in several genetic backgrounds. **(A)** DNA damage sensitivity analysis of *rtt105*Δ mutant cells in various genetic backgrounds. 10-fold serial dilutions of the indicated cells were spotted on YPD control or drug-containing YPD plates. All plates were imaged after 2 or 3 days of incubation at 30ºC. **(B)** Western Blotting analysis of *rtt105*Δ mutant cells in various genetic backgrounds. Whole cell extracts of indicated yeast strains were subjected to immunoblotting detected by antibodies against Rtt105. Ponceau S staining was used as a loading control. **(C)** To perform Rtt105 rescue assays, full length Rtt105 under the control of its own promoter was cloned into the pRS316 expression vector and then transformed into *rtt105*Δ (W303) mutant cells. Cells expressing either a vector control (vc) or full length *RTT105* were diluted, as above, and spotted on selective growth media (SCM-Ura) with or without the indicated DNA damage agents.

Appendix Figure S2

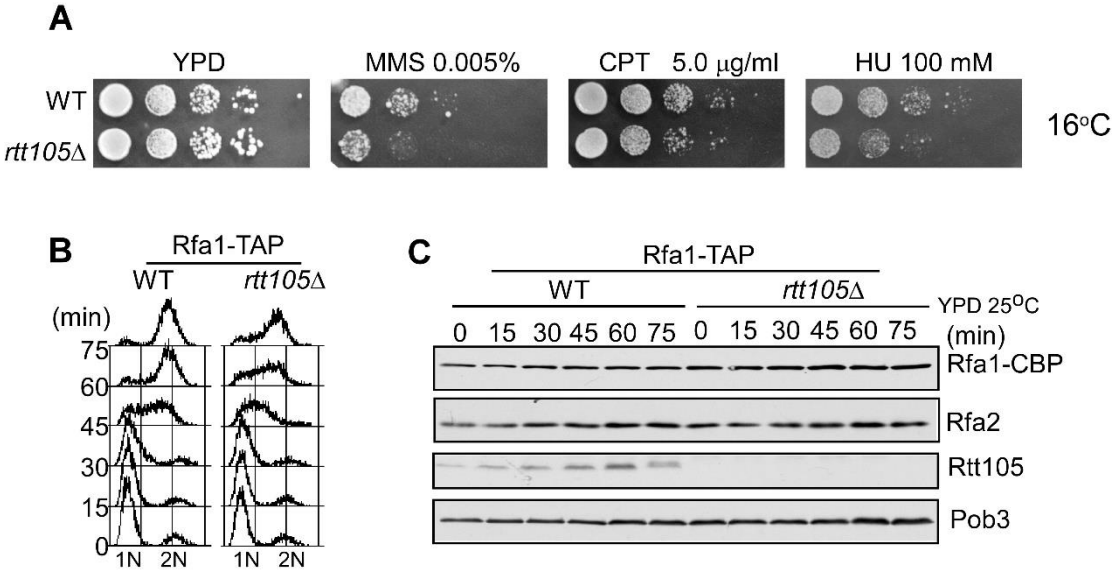

Fig S2. Analysis of cell cycle progression in *rtt105*Δ cells. (A) DNA damage sensitivity analysis of *rtt105*Δ mutant cells grow at 16°C. The dot assay was performed as in Fig S1A. All plates were imaged after 5 to 8 days of incubation at 16°C. **(B)** FACS analysis of the cell cycle progression profile of samples for ChIP experiments shown in Fig 2F. **(C)** Whole cell extracts of the samples for ChIP experiments shown in Fig 2F were immunoblotted with antibodies against CBP, Rfa2, Rtt105, and Pob3. Pob3 (a subunit of FACT) was used as a loading control.

Appendix Figure S3

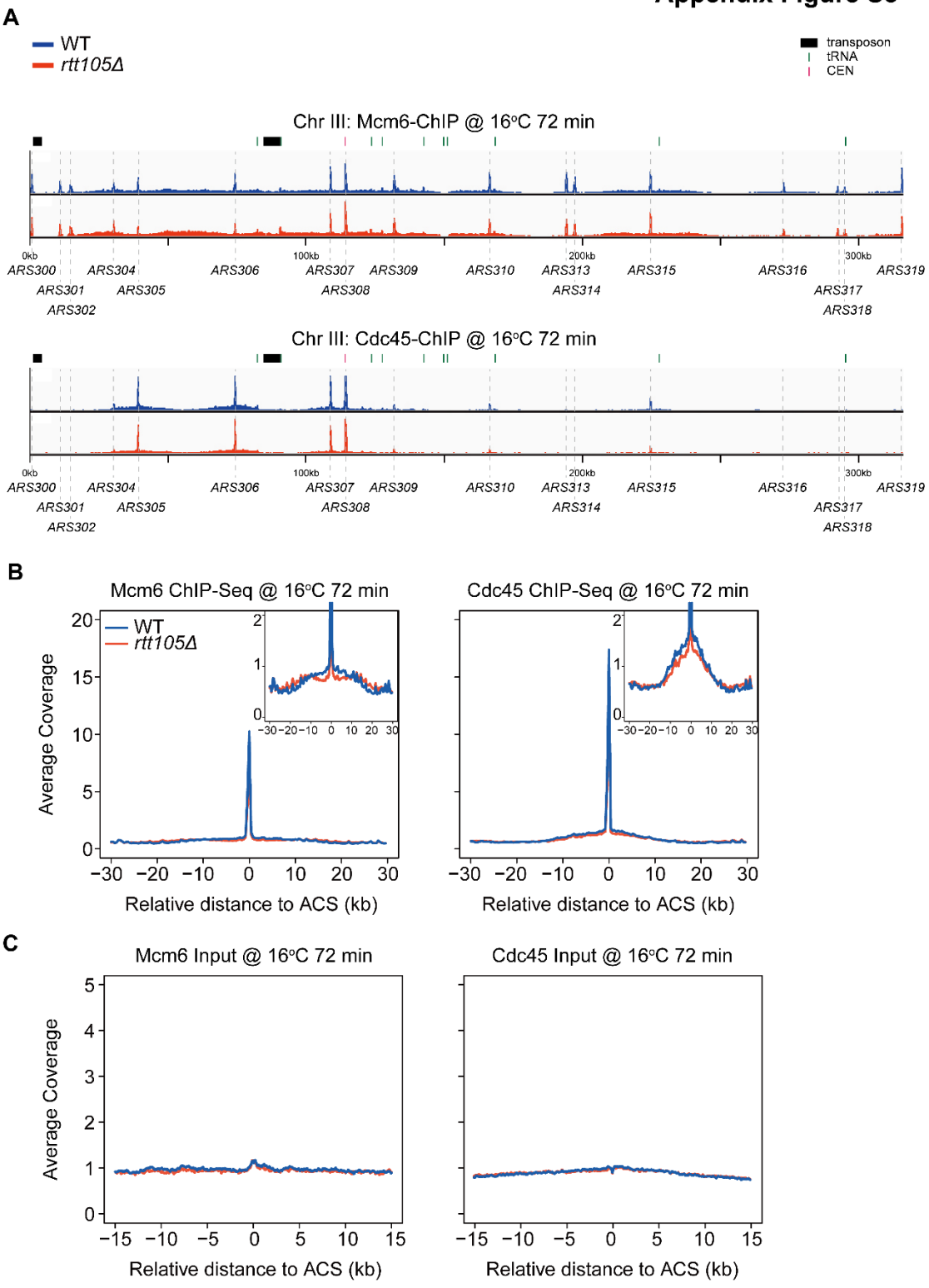

Fig S3. Genome wide analysis of the chromatin binding of Cdc45 and Mcm6 during S phase in *rtt105*Δ cells. (A) Snap shot of Mcm6 (top) and Cdc45 (bottom) ChIP-Seq at Chromosome III at S phase without HU treatment (16 ºC 72 min). The sequencing reads were mapped to the yeast reference

genome. **(B)** The average Mcm6 (left) and Cdc45 (right) ChIP-Seq read density from cells released into 16ºC for 72 min around ACS sites are shown. **(C)** The average read density around ACS sites of input samples for ChIP-Seq samples is shown.

Appendix Fig S4

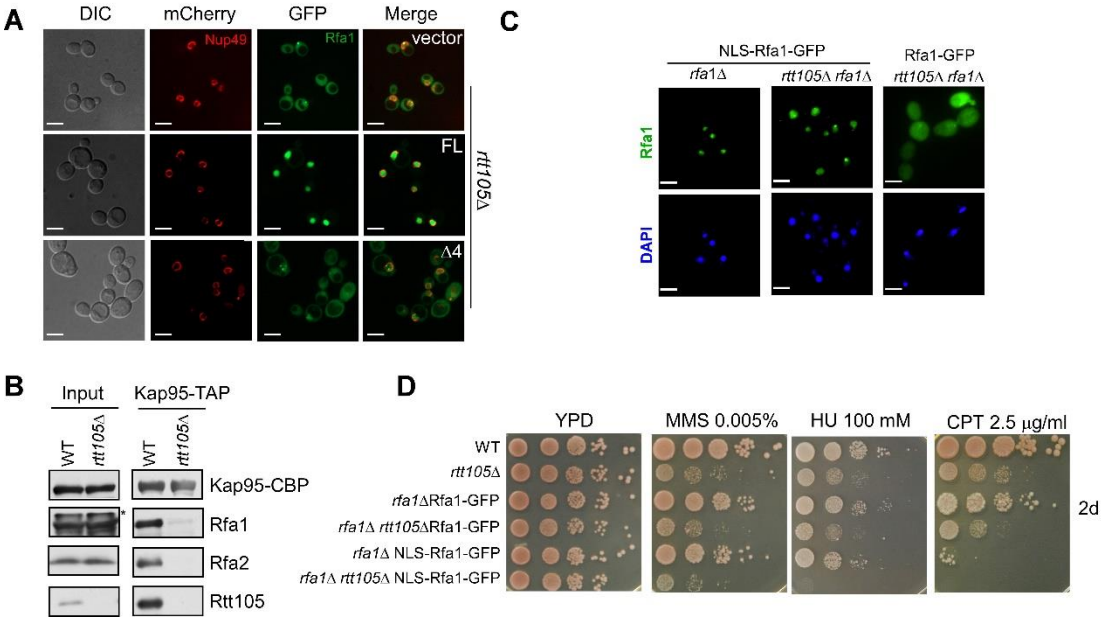

Fig S4. Rtt105 mediates the nuclear import of RPA. (A) The C-terminus deletion of Rtt105 cannot rescue the nuclear localization defect of Rfa1-GFP in *rtt105*Δ cells. Plasmid-expressed full-length and C-terminus truncated form (Δ4) of Rtt105 were transformed into the *rtt105*Δ strain and cultured for fluorescent microscopy. Rfa1-GFP is shown in green. Nuclear envelope was visualized with Nup49-mCherry and shown in red. DIC: differential interference contrast. FL: full-length Rtt105; Δ4: truncated Rtt105 Δ4 (Δ155-208). **(B)** Rtt105 is important for the interaction between Kap95 and the RPA complex. Tap-tagged Kap95 was purified from yeast cells, and the resulting protein complexes were analyzed by Western blotting using antibodies against CBP, Rfa1, Rfa2, and Rtt105. Protein levels were analyzed in the input cell extracts as a control.* Non-specific band. **(C)** Nuclear localization sequence allows Rfa1 to enter nuclear in *rtt105*Δ cells. The WT *RFA1* gene was fused with an SV40 large T Antigen nuclear localization sequence (NLS) at its 5'-end and a GFP gene at its 3' end to obtain a construct, driven by the *RFA1* promoter to express the

NLS-RFA1-GFP fusion protein. The engineered construct was then transformed into WT or *rtt105*Δ mutant yeast cells to replace its endogenous *RFA1* expression. The resulting yeast cells were then visualized under microscopy. RFA1-GFP lacking the NLS sequence was transformed into *rtt105*Δ *rfa1*Δ cells as a control. DAPI staining indicates nuclear DNA. **(D)** NLS-fused Rfa1 does not rescue the DNA damage sensitivity of *rtt105*Δ cells. Please note that Rfa1-GFP and NLS-Rfa1-GFP are likely not fully functional. Therefore, both show some additive/synthetic defects with the *rtt105*Δ mutant. Ten-fold serial dilution of yeast cells of the indicated genotypes were assayed on normal growth media (YPD) and on media containing the indicated concentrations of DNA damaging agents. Cells were imaged after 2 days of incubation at 30°C.

Appendix Figure S5

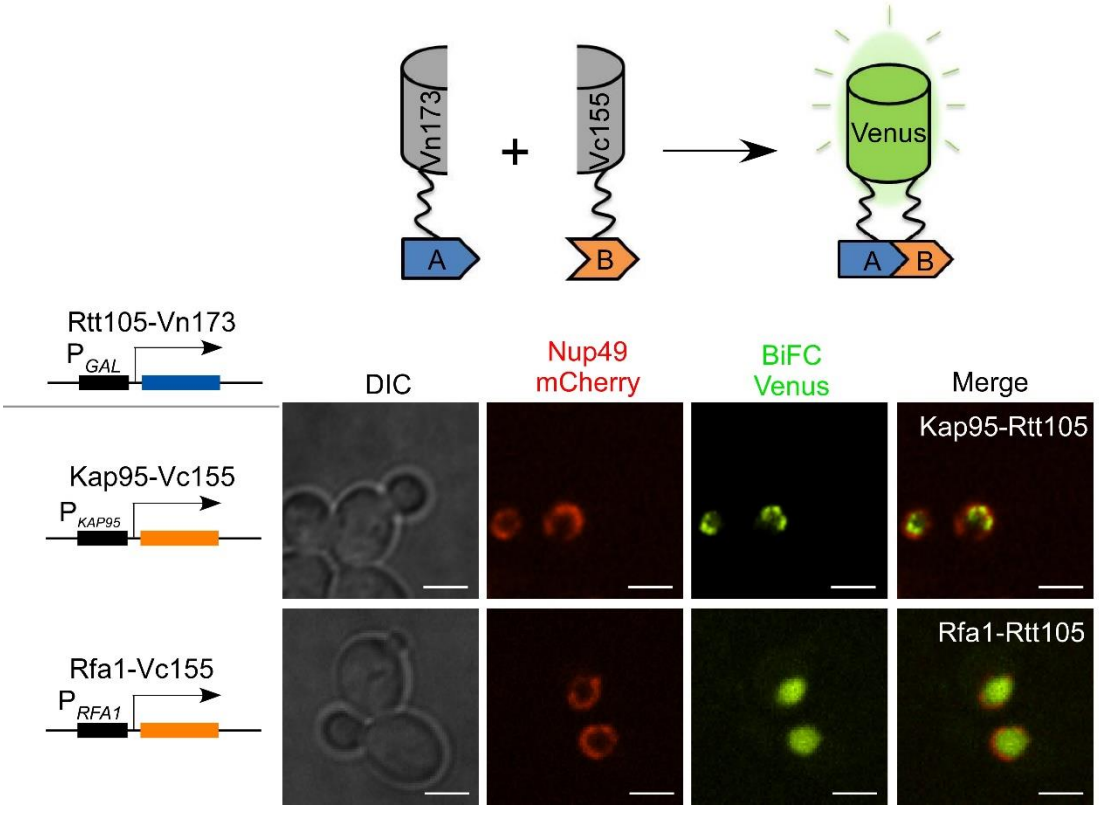

Fig S5. The Kap95-Rtt105 interaction mainly occurs at nuclear periphery regions while the Rfa1-Rtt105 mainly occurs within nuclear. Bimolecular Fluorescence Complementation (BiFC) assay to visualize protein-protein interactions in living yeast cells is illustrated (Top panel). N-terminal fragment

of Venus fluorescent protein was fused to Rtt105 (Rtt105-Vn173) and C terminal fragment of Venus was fused to Kap95 or Rfa1 (Kap95-Vc155 or Rfa1-Vc155) separately. Interactions of Kap95 with Rtt105 or Rfa1 with Rtt105 will bring the fluorescent fragments within proximity, allowing the reporter protein to reform in its native structure and emit its fluorescent signal.

Appendix Figure S6

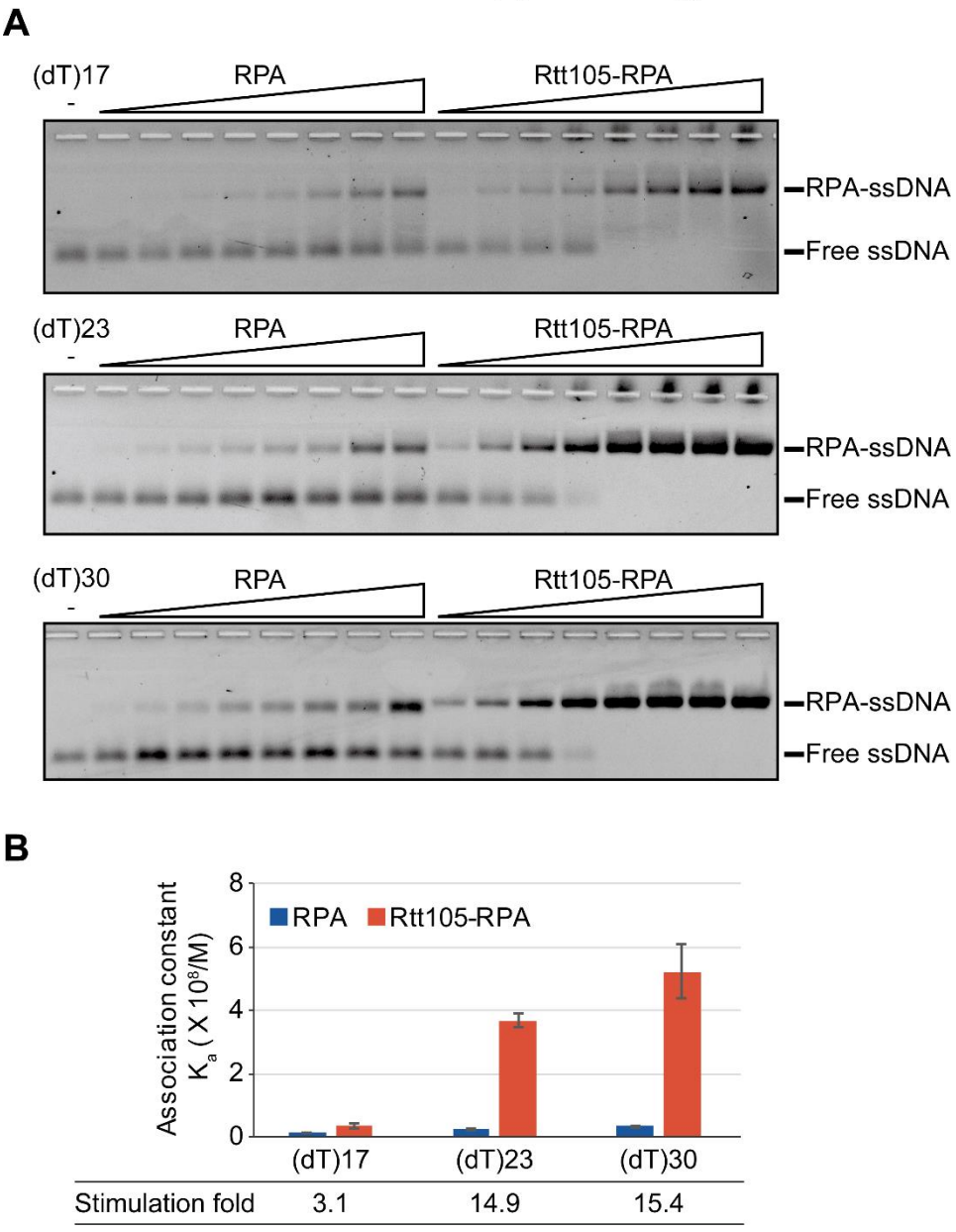

Fig S6. Rtt105 promotes RPA binding to ssDNA *in vitro*. (A) An electrophoresis mobility shift (EMSA) assay was performed to compare the ssDNA binding capacity of RPA with that of the Rtt105-RPA complex in various length of ssDNA substrates. Cy3-labeled Oligo(dT)s were used as the substrate

in this assay. The reaction mixtures were resolved on native gels, and the Cy3 signals were detected on a Typhoon FLA 9500 imager. At least three independent biological repeats were performed, and similar results were obtained each time. **(B)** Comparison of association constants (Ka). The apparent binding constants of RPA and Rtt105-RPA to different length of oligo(dT)s are presented graphically. The average apparent association constants from at least three independent titrations±SD. The stimulatory effect of Rtt105 on RPA binding was determined by calculating the fold Ka change for each indicated length of oligo(dT). (i.e.: stimulatory effect of Rtt105 = Ka of RPA with Rtt105 / Ka of RPA alone.)

Appendix Figure S7

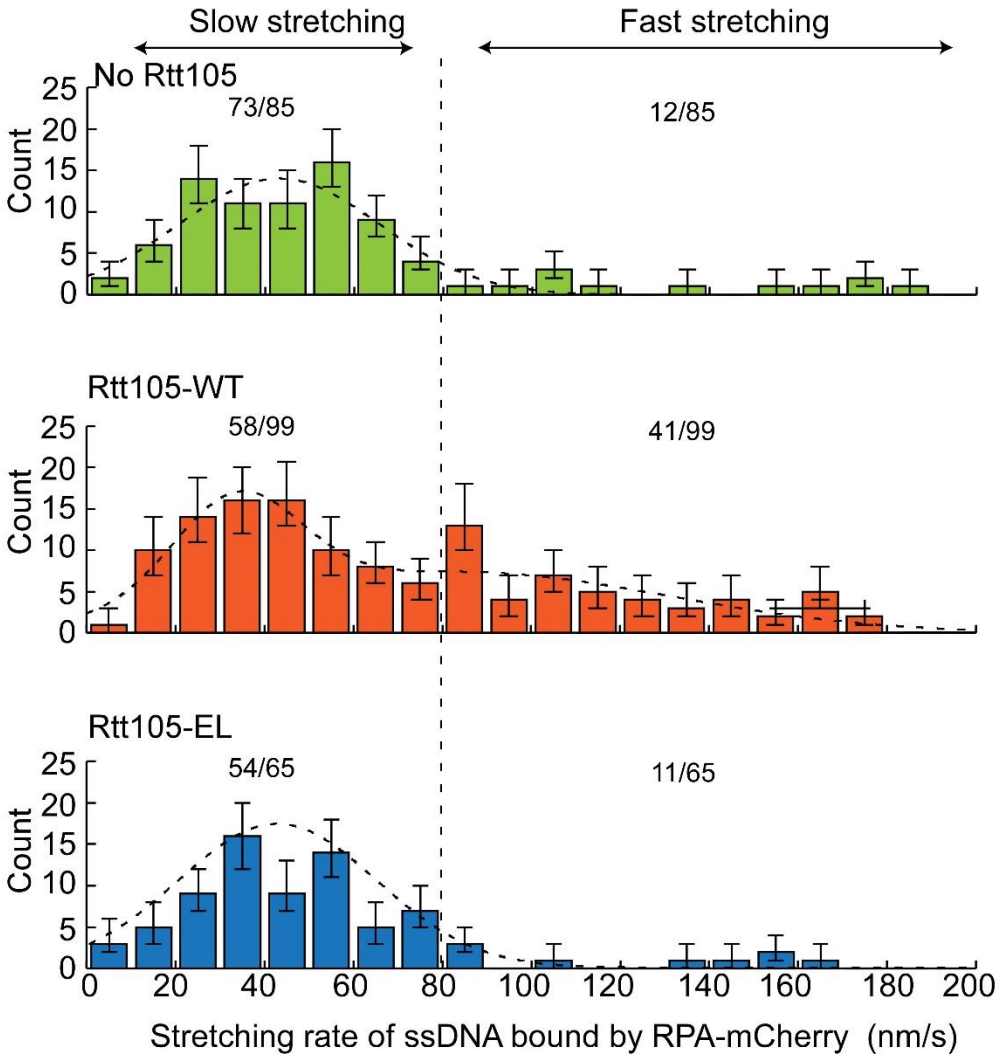

Fig S7. The stretching of ssDNA bound by RPA-mCherry can be categorized into slow and fast stretching patterns. The stretching rates defined by the length change of ssDNA bound by RPA-mcherry in unit time (nm/s) were measured from each kymographs as shown in Fig 5B (White arrows), and then they were plotted in histograph. Single-Gaussian function was used to fit the cases of 5 nM RPA-mCherry without Rtt105 or with Rtt105-EL mutant proteins. Double- Gaussian functions were used to fit the case of 5 nM RPA-mCherry with 5 nM Rtt105-WT and the cutoff of 80 nm/s was determined by plotting a dash line between two Gaussian peaks in this data set. Slow stretching event was defined as the rate was less than 80 nm/s, and the fast stretching event was greater than 80 nm/s. The error bars for all rate distributions represent 70% confidence intervals obtained through bootstrap analysis.

Appendix Figure S8

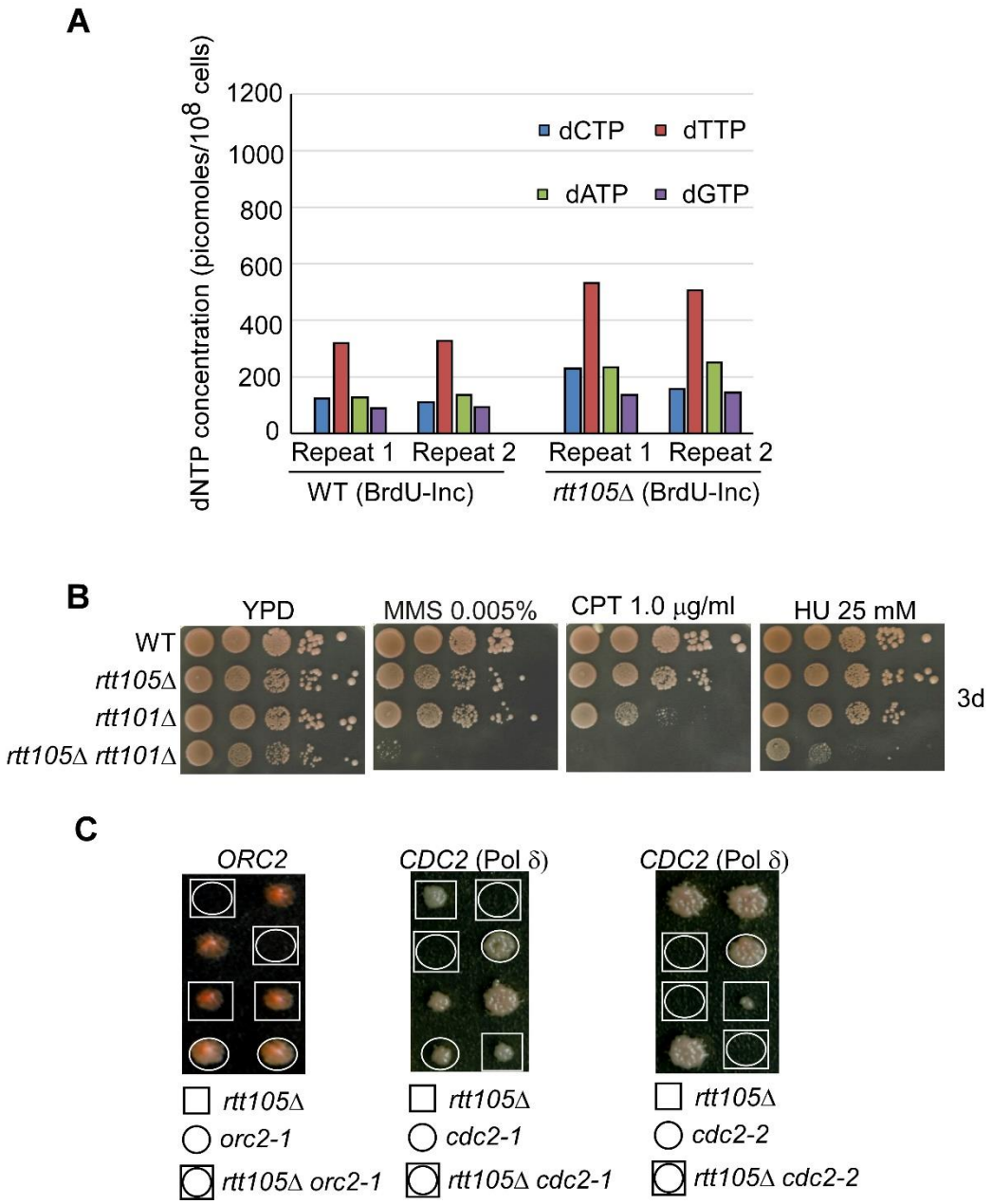

Fig S8. Cells lacking Rtt105 showed increased cellular dNTP levels and increased DNA damage sensitivity. (A) Measurement of dNTP levels in WT and *rtt105*Δ strains. Levels of dNTPs in logarithmically growing asynchronized cells were measured in BrdU-incorporated (BrdU-Inc) WT and *rtt105*Δ strains by HPLC. **(B)** Combining the *RTT105* deletion with deletions of *RTT101* leads to increased sensitivity to HU, CPT and MMS. Yeast spot assays were performed as in Fig 6H. **(C)** Tetrad analysis of the meiotic progeny of diploid strains was performed in indicated genotypes. Dissected tetrad spores were

grown on YPD plates for 3 days before taking pictures.

Appendix Figure S9

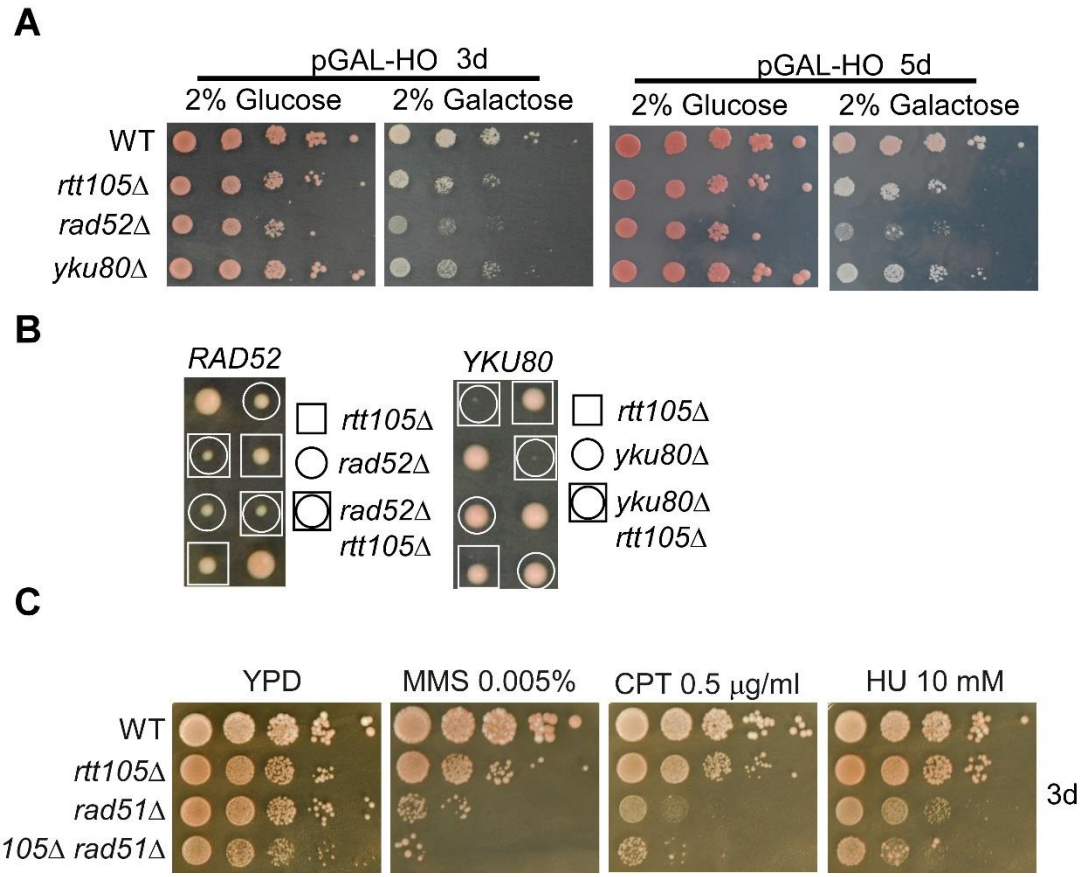

Fig S9. Rtt105 is important for maintaining genome stability. (A) *rtt105*Δ cells were sensitive to HO-induced double strand breaks (DSBs). Indicated strains harboring the p*GAL-HO* plasmid were spotted onto either 2% glucose or 2% galactose-containing SCM–URA plates in 10-fold serial dilutions. All plates were imaged after 3 to 5 days of incubation at 30°C. **(B)** Tetrad analysis of the meiotic progeny of diploid strains was performed in indicated genotypes. Dissected tetrad spores were grown on YPD plates for 3 days before taking pictures. **(C)** Combining the *RTT105* deletion with deletions of *RAD51* leads to increased growth defect and increased sensitivity to HU, CPT and MMS. Yeast spot assays were performed as in Fig 6H.

Table S1: Yeast strains used in this study (Isogenic with W303)

Name	Genetic background	Reference
W303-1a	*MATa leu2-3, 112 ura3-1 his3-11,15, trp1-1, ade2-1, can1-100*	(Thomas & Rothstein, 1989)
W303-1α	*MATα leu2-3, 112 ura3-1 his3-11,15, trp1-1, ade2-1, can1-100*	(Thomas and Rothstein, 1989)
LQY1638	*MATa leu2-3,112 ura3-1 his3-11,15, trp1-1, ade2-1, can1-100, rtt105Δ::natR*	This study
LQY1981	*MATα leu2-3, 112 ura3-1 his3-11,15, trp1-1, ade2-1, can1-100, rtt105Δ::natR*	This study
LQY1995	*MATa leu2-3, 112 ura3-1 his3-11,15, trp1-1, ade2-1, can1-100, rtt101Δ:: kanMX6, rtt105Δ::natR*	This study
LQY1676	*MATa leu2-3, 112 ura3-1 his3-11,15, trp1-1, ade2-1, can1-100,rtt105Δ::natR, cac1Δ::leu2, rtt106Δ::kanMX6*	This study
LQY1349	*MATa leu2-3, 112 ura3-1 his3-11,15, trp1-1, ade2-1, can1-100, rtt109Δ:: kanMX6, rtt105Δ::natR*	This study
LQY1431	*MATα leu2-3, 112 ura3-1 his3-11,15, trp1-1, ade2-1, can1-100, rtt105-TAP::TRP1*	This study
LQY1400	*MATα leu2-3, 112 ura3-1 his3-11,15, trp1-1, ade2-1, can1-100, rtt105-5Flag:: natR*	This study
LQY1826	*MATa leu2-3, 112 ura3-1 his3-11,15, trp1-1, ade2-1, can1-100, rfa2-TAP::TRP1, rtt105Δ:: kanMX6*	This study
LQY1856	*MATa leu2-3, 112 ura3-1 his3-11,15, trp1-1, ade2-1, can1-100, rfa1-TAP::TRP1, rtt105Δ:: natR*	This study
LQY1857	*MATα leu2-3, 112 ura3-1 his3-11,15, trp1-1, ade2-1, can1-100, rfa1-TAP::TRP1, rtt105Δ:: natR*	This study
LQY1982	*MATa leu2-3, 112 ura3-1 his3-11,15, trp1-1, ade2-1, can1-100, rfa3-TAP::TRP1, rtt105Δ:: natR*	This study
SBY102	*MATa leu2-3, 112 ura3-1 his3-11,15, trp1-1, ade2-1, can1-100, rfa1-1::TRP1，pJM114-rfa1-URA*	(Kim & Brill, 2001)
LQY2813	*MATa leu2-3, 112 ura3-1 his3-11,15, trp1-1, ade2-1, can1-100, rtt105Δ:: natR, rfa1-1::TRP1，pJM114-rfa1-URA*	This study
LQY2097	*MATa leu2-3, 112 ura3-1 his3-11,15, trp1-1, ade2-1, can1-100, rfa1-GFP::kanMX6*	This study
LQY2098	*MATa leu2-3, 112 ura3-1 his3-11,15, trp1-1, ade2-1, can1-100, rfa2-GFP::kanMX6*	This study
LQY2111	*MATa leu2-3,112 ura3-1 his3-11,15, trp1-1, ade2-1, can1-100, rtt105Δ:: natR, rfa1-GFP::kanMX6*	This study
LQY2112	*MATa leu2-3,112 ura3-1 his3-11,15, trp1-1, ade2-1, can1-100, rtt105Δ:: natR, rfa2-GFP::kanMX6*	This study
LQY2115	*MATa leu2-3,112 ura3-1 his3-11,15, trp1-1, ade2-*	This study

	1, can1-100, rtt105Δ:: natR, rfa1-1::TRP1 , pRS313-RFA1-HIS	
LQY2151	*MATa leu2-3, 112 ura3-1 his3-11,15, trp1-1, ade2-1, can1-100, nup49-mCherry::URA*	This study
LQY2184	*MATα leu2-3, 112 ura3-1 his3-11,15, trp1-1, ade2-1, can1-100, nup49-mCherry::URA*	This study
LQY2200	*MATa leu2-3,112 ura3-1 his3-11,15, trp1-1, ade2-1, can1-100, rtt105Δ::natR, nup49-mCherry::URA*	This study
LQY2263	*MATa leu2-3,112 ura3-1 his3-11,15, trp1-1, ade2-1, can1-100, rad52-eGFP:: kanMX6*	This study
LQY2274	*MATa leu2-3,112 ura3-1 his3-11,15, trp1-1, ade2-1, can1-100, rtt105Δ::natR, rad52-eGFP:: kanMX6*	This study
LQY2774	*MATa leu2-3,112 ura3-1 his3-11,15, trp1-1, ade2-1, can1-100, nup49-mCherry::URA, rad52-eGFP:: kanMX6*	This study
LQY2775	*MATa leu2-3,112 ura3-1 his3-11,15, trp1-1, ade2-1, can1-100, rtt105Δ:: natR, nup49-mCherry::URA, rad52-eGFP:: kanMX6*	This study
LQY658	*MATa leu2-3,112 ura3-1 his3-11,15, trp1-1, ade2-1, can1-100, p306-BrdU-Inc::URA*	This study (p306–BrdU–Inc plasmid was a gift from Dr. Oscar Aparicio) (Viggiani & Aparicio, 2006)
LQY2185	*MATa leu2-3,112 ura3-1 his3-11,15, trp1-1, ade2-1, can1-100, rtt105Δ::natR, p306-BrdU-Inc::URA*	This study
LQY2610	*MATa leu2-3,112 ura3-1 his3-11,15, trp1-1, ade2-1, can1-100, rfa1-1::Trp, pRS313-rfa1-Vc155::Leu2*	This study
LQY2611	*MATa leu2-3,112 ura3-1 his3-11,15, trp1-1, ade2-1, can1-100, rtt105Δ::natR, rfa1-1::Trp, pRS313-rfa1-Vc155::Leu2*	This study
LQY2717	*MATa leu2-3,112 ura3-1 his3-11,15, trp1-1, ade2-1, can1-100, kap95-TAP::TRP1*	This study
LQY27	*MATa leu2-3,112 ura3-1 his3-11,15, trp1-1, ade2-1, can1-100, kap95-TAP::TRP1*	This study
LQY2810	*MATa leu2-3,112 ura3-1 his3-11,15, trp1-1, ade2-1, can1-100, rfa1-1::Trp, pRS413-NLS-rfa1-GFP::HIS*	This study
LQY2811	*MATa leu2-3,112 ura3-1 his3-11,15, trp1-1, ade2-1, can1-100, rtt105Δ::natR, rfa1-1::Trp, pRS413-NLS-rfa1-GFP::HIS*	This study
LQY2812	*MATα leu2-3,112 ura3-1 his3-11,15, trp1-1, ade2-*	This study

	1, can1-100, rtt105Δ::natR, rfa1-1::Trp, pRS413-NLS-rfa1-GFP::HIS	
LQY3976	*MATa leu2-3,112 ura3-1 his3-11,15, trp1-1, ade2-1, can1-100, rad51Δ::TRP1*	This study
LQY3986	*MATa leu2-3,112 ura3-1 his3-11,15, trp1-1, ade2-1, can1-100, rtt105Δ::natR, rad51Δ::TRP1*	This study

Table S2: Primers and oligoes used in this study.

Name	Sequence	Application
ARS607(F)	tgccgcacgccaaacattgc	Real Time PCR
ARS607(R)	cggctcgtgcattaagcttg	Real Time PCR
ARS607+14kb(F)	ctcttcatcactggagtcct	Real Time PCR
ARS607+14kb(R)	cggctgtcatgccaagatgc	Real Time PCR
ARS305(F)	agcaagaccggccagtttga	Real Time PCR
ARS305(R)	gcactttgatgaggctctagcaa	Real Time PCR
ARS501(F)	gaatgtgtctacgtaattgg	Real Time PCR
ARS501(R)	cctttcttttggagctgtca	Real Time PCR
ARS305+12kb *(F)*	gcggaagtctttgcaactgatatg	Real Time PCR
ARS305+12kb *(R)*	tgcttgatttcttcgcagtattgg	Real Time PCR
Rtt105 deletion-natR (F)	caaaatacagtcaaagagtttagctcggaaacatggaggcccagaataccc	*rtt105Δ::natR* Construction
Rtt105 deletion-natR(R)	agggctatttctgtaatagcaatgatgccacagtatagcgaccagcattcac	*rtt105Δ::natR* Construction
Rtt105-TAP (F)	aataaaaatgtttatgagaacaactcgtatccgaactctcatacgtccatggaaaagagaag	Rtt105-TAP Construction
Rtt105-TAP (R)	taaatatgacaggctagggctatttctgtaatagcaatgatgccatacgactcactataggg	Rtt105-TAP Construction
Rfa1-flag (F)	gaagccgactatcttgccgatgagttatccaaggctttgttagct cggatccccgggttaattaa	Rfa1-5Xflag Construction
Rfa1-flag (R)	tctcatatgttacatagattaaatagtacttgattatttgatacagaattcgagctcgtttaaac	Rfa1-5Xflag Construction
Rtt105-FL-pET21a (F)	cgggatccatgtacagcaatcataa	pET21a-Rtt105-His construction
Rtt105-FL-pET21a (R)	ccctcgagcgtatgagagttcgga	pET21a-Rtt105-His construction
Rtt105-dC-pET21a	ccctcgagtcaatattcagccatgtcagagg	pET21a-Rtt105-

(R)		dC-His construction
GST-Rtt105 Δ(2-52) (F)	ccgcgtggatccatg caacaaagtggcac	GST-Rtt105 truncation purification
GST-Rtt105 Δ(2-52) (R)	gtgccactttgttg catggatccacgcgg	GST-Rtt105 truncation purification
GST-Rtt105 Δ(53-103) (F)	cagaagagaacaaa ttggagtccatgag	GST-Rtt105 truncation purification
GST-Rtt105 Δ(53-103) (R)	ctcatggactccaa tttgttctcttctg	GST-Rtt105 truncation purification
GST-Rtt105 Δ(104-154) (F)	gatcagagatcacgg atggctgaatatatg	GST-Rtt105 truncation purification
GST-Rtt105 Δ(104-154) (R)	catatattcagccat ccgtgatctctgatc	GST-Rtt105 truncation purification
GST-Rtt105 Δ(155-208) (F)	gctctaccctctgac tgactcgagcggccg	GST-Rtt105 truncation purification
GST-Rtt105 Δ(155-208) (R)	cggccgctcgagtca gtcagagggtagagc	GST-Rtt105 truncation purification
Rtt105-promoter(F)	ccctcgagtcacgtatgagagttc	pRS316-Rtt105 construction
Rfa1-GFP (F)	actatcttgccgatgagttatccaaggctttgttagct gccgccgcaggtgacggt	Rfa1-GFP construction
Rfa1-GFP (R)	gttacatagattaaatagtacttgattatttgataca gaattcgagctcgtttaaac	Rfa1-GFP construction
Rfa2-GFP (F)	caacttttgatgacaataacttctttgcccta gccgccgcaggtgacggt	Rfa2-GFP construction
Rfa2-GFP (R)	agaaatgctaaaaaaataatctatatattt gaattcgagctcgtttaaac	Rfa2-GFP construction
Rad52-GFP (F)	caaagatcaatcccctgcatgcacgcaagcctact gccgccgcaggtgacggt	Rad52-GFP construction
Rad52-GFP (R)	atgcaaatttttttatttgtttcggccaggaagcgttgaattcga gctcgtttaaac	Rad52-GFP construction
Nup49-mCherry (F)	catcaaaaaacgaaaacactggcatcattgagcataggt gacggtgctggttta	Nup49-mCherry construction
Nup49-mCherry (R)	tgttatacgcactatataaactttcagggcgatttactcgatg aattcgagctcg	Nup49-mCherry construction

NLS-Rfa1-GFP (F)	cgggatcc atg ccgaaaaaaaaacgcaaagtgcgctctaatgttattccctc	NLS-Rfa1-GFP tagging plasmid construction
NLS-Rfa1-GFP (R)	gcgtcgacttatttgtacaattcatcaatac	NLS-Rfa1-GFP tagging plasmid construction
pRS313-Vn173 (F)	cgggatcc ggaggtggaggttcaggaggtggaggttca atggtgagcaagggcg	pRS313-Vn173 plasmid construction (BamHI/SalI)
pRS313-Vn173 (R)	gcgtcgac gatgttgtggcggatcttga	pRS313-Vn173 plasmid construction (BamHI/SalI)
pRS314-Vc155 (F)	ccaagctt ggaggtggaggttcaggaggtggaggttca gccgacaagcagaagaa	pRS314-Vn173 plasmid construction (BamHI/SalI)
pRS314-Vc155 (R)	gcgtcgac ttacttgtacagctcgtccat	pRS314-Vn173 plasmid construction (BamHI/SalI)
Rfa1-ΔN (F)	cgggatcccgtgctgatatggtcaacca	Rfa1 truncation expression
Rfa1-ΔN (R)	ccctcgagttaagctaacaaagccttgg	Rfa1 truncation expression
Rfa1-ΔC (F)	cgggatcc atgagcagtgttcaactttcga	Rfa1 truncation expression
Rfa1-ΔC (R)	ccctcgag agtaatacgctgagcaatgaat	Rfa1 truncation expression
Rfa1-ΔAB (overlap-F1)	cgggatcc atgagcagtgttcaactttcga	Rfa1 truncation expression
Rfa1-ΔAB (overlap-R1)	aaagtgatgaagtttgcgtt ttgcgaattagggttttcattg	Rfa1 truncation expression
Rfa1-ΔAB (overlap-F2)	ccctaattcgcaaaaa caacgcaaacttcatcacttta	Rfa1 truncation expression
Rfa1-ΔAB (overlap-R2)	ccctcgag ttaagctaacaaagccttggat	Rfa1 truncation expression
Rfa1-N (F)	cgggatcc atgagcagtgttcaactttcga	Rfa1 truncation expression
Rfa1-N (R)	ccctcgag tttttgcgaattagggtttt	Rfa1 truncation expression
Rfa1-AB (F)	cgggatcc agaccaatttttgccatcga	Rfa1 truncation expression

Rfa1-AB (F)	ccctcgag ggaatcataccaacccttaag	Rfa1 truncation expression
blunt-end XO-1	acgctgccgaattctaccagtgccttgctaggacatctttgc ccacctgcaggttcaccc	EMSA substrate generation
blunt-end XO-2	gggtgaacctgcaggtgggcaaagatgtccatctgttgtaa tcgtcaagctttatgccgt	EMSA substrate generation
5' Cy3-ssDNA-30nt	Cy3-cgataagcttgatatcgaattcctgcagcc	EMSA substrate(Zou & Elledge, 2003)
rad51_pFA6a-f	tagttatttgttaaaggcctactaatttgttatcgtcatccagct gaagcttcgtacgc	*rad51Δ::TRP1* Construction
rad51_pfa6a-r	taaacctgtgtaaataaatagagacaagagaccaaatac gcataggccactagtggatc	*rad51Δ::TRP1* Construction
(dT)17	Cy3-TTTTTTTTTTTTTTTTT	*EMSA*
(dT)23	Cy3-TTTTTTTTTTTTTTTTTTTTTTT	*EMSA*
(dT)30	Cy3-TTTTTTTTTTTTTTTTTTTTTTTTTTTTTT	*EMSA*
VC155-F	cggtggcggccgccttgtac	*pRS315-KAP95-Vc155 plasmid construction*
VC155-R	agctggatccggaggtggag	*pRS315-KAP95-Vc155 plasmid construction*
pro-KAP95-F	acgcgtcgac ggttggcatgccaaaggaag	*pRS315-KAP95-Vc155 plasmid construction*
pro-KAP95-R	cgggatcc taaggataattgacgcttct	*pRS315-KAP95-Vc155 plasmid construction*

Supplementary Materials and Methods:

Constructing *RTT105* deletion mutant

RTT105 deletion at its endogenous chromosome locus was introduced by homologous-recombination-based standard PCR engineering. We verified the *rtt105*Δ mutant strain by sequencing ranging from upstream 1 kb and downstream 1 kb of Rtt105 chromosome locus region (Chromosome V 366802...367428) and validated its removal without introducing any point mutation or shift of its open reading frame (ORF). Deletion of Rtt105 is also verified by western blot against Rtt105 antibody (ABclonal, generated from recombinant protein) prior to performing subsequent experiments.

Plasmid construction

All plasmids are constructed by common sub-cloning strategy. For NLS-tagging experiments, full length *RFA1* coding sequence were fused with a monopartite SV40 large T Antigen nuclear localization sequence (NLS) (PKKKRKV) at its 5'-end and a GFP coding sequence at its 3' end to obtain a NLS-RFA1-GFP fusion proteins driven by *RFA1* promoter. The primers and oligos used in this study were listed in Appendix Table S2.

Tandem affinity purification (TAP)

TAP-tagged purifications were performed as described(Li et al, 2008; Puig et al, 2001). Briefly, exponentially growing yeast cells were harvested by centrifugation and washed with 10% glycerol. Yeast cells were resuspended in an equal volume of buffer A (25 mM Tris, pH 8.0, 100 mM NaCl, 1 mM EDTA, 10 mM $MgCl_2$, 0.01% NP40) with protease inhibitors (1 mM DTT, 1 mM PMSF, 1 mM Benzamidine, 1 mM Pefabloc) and 15 kU/ml DNase I and freezed in liquid nitrogen. Frozen cells were ground in freezer mill (SPEX SamplePrep^{LLC} 6870). Cell lysates were clarified by centrifugation (20,450 g, 40 minutes) and then incubated with IgG sepharose beads (GE healthcare) for 2 hours. IgG bound

proteins were digested with TEV protease after extensive washing for 3 hours at 16℃. The resulted proteins were further bound with calmodulin beads (Agilent Technologies), eluted with SDS sample buffer, resolved on SDS-PAGE gels and detected by Western blotting.

***In vitro* pull-down assay**

To purify protein with glutathione S-transferase (GST) tag, coding sequence of Rtt105 and its truncations was introduced into expression vector pGEX-4T-1(GE Healthcare). Confirmed after sequencing, the constructs were transformed into *E.coli* strain BL21 (DE3). GST-tagged proteins were induced by adding 0.1 mM IPTG at 18℃ overnight and purified using Glutathione agarose (GE Healthcare) eluted in 100 mM reduced glutathione (Sigma).

To purify protein with histidine (His) tag, coding sequence of Rtt105 was introduced into expression vector pET21a (Novagen). Confirmed after sequencing, the constructs were transformed into *E.coli* strain BL21 (DE3) and Rosetta. His-tagged proteins were induced by adding 1 mM IPTG at 18℃ overnight and purified using Ni-NTA agarose beads (Qiagen) eluted in 300 mM imidazole (Sigma).

To purify proteins with Maltose Binding Protein (MBP) tag, coding sequences of Rtt105, Rtt105 truncations, Rfa1, Rfa1 truncation forms, Rfa2 and Rfa3 were introduced into expression vector pLM302. Truncated forms of Rfa1 were designed based on previous structural research(Fan & Pavletich, 2012; Park et al, 2005).Confirmed after sequencing, the constructs were transformed into *E.coli* strain BL21(DE3). MBP-tagged proteins were induced by adding 1 mM IPTG at 18℃ overnight and purified using amylose agarose beads (Qiagen) eluted in maltose elution buffer (1XPBS, pH 7.5 with 10 mM Maltose,10% glycerol, 0.1% Triton and 1 mM DTT).

To purify RPA complex for *in vitro* Pull-down, Rfa1/Rfa1 N terminus

truncated coding sequence was constructed on pGEX-4T-1 with GST tag. Rfa2 and Rfa3 subunits were introduced into pCDF-Duet (Novagen) plasmid with His-tagged at the N terminal of Rfa2. Two verified constructs were transformed into *E.coli* strain BL21 (DE3) simultaneously. Purification of intact RPA complex was performed as described previously (Binz et al, 2006).

For GST pull-down, 30 μg GST, GST-Rtt105 or GST-truncated Rtt105 was first incubated with Glutathione agarose (GE healthcare) in buffer A100 (25 mM Tris-HCl pH 7.5, 100 mM NaCl, 1 mM EDTA and 0.01% Triton X-100) at 4℃ for no more than 4 hours . After extensive washing, protein-bound beads were separated into equal amount and incubated with indicated amount of proteins fusing other affinity tags in buffer A100 at 4℃ overnight. Beads were washed extensively in buffer A 200 (25 mM Tris-HCl, pH 7.5, 200 mM NaCl, 1 mM EDTA and 0.01% Triton X-100). Protein-bound beads were eluted with SDS sample buffer, resolved by SDS-PAGE and detected by Coommassie Brilliant Blue (CBB) Staining or Silver Staining.

For MBP pull-down, 30 μg MBP or MBP-Rtt105 was first incubated with Amylose agarose (Qiagen) in buffer A200 (25 mM Tris-HCl pH 7.5, 200 mM NaCl, 1 mM EDTA and 0.01% Triton X-100) at 4℃ for 4 hours. After extensive washing, protein-bound beads were separated into equal amount and incubated with indicated amount of proteins fusing other affinity tags in buffer A200 at 4℃ overnight. Beads were washed extensively in buffer A 300 (25 mM Tris-HCl pH 7.5, 300 mM NaCl, 1 mM EDTA and 0.01% Triton X-100). Protein-bound beads were eluted with SDS sample buffer, resolved by SDS-PAGE and detected by Coommassie Brilliant Blue (CBB) Staining or Silver Staining.

Chromatin immunoprecipitation-quantitative PCR assay (ChIP-qPCR)

Briefly, exponentially growing cells (*MATa*) were synchronized with 5 μg/ml α-factor for 3 hours at 25℃ and then released into YPD with or without 200

mM Hydroxyurea (sigma). Samples were collected at the indicated time points or temperatures for following ChIP assay. Procedure of following ChIP was described previously(Nelson et al, 2006) with minor modification based on special requirement. Cell samples were incubated with 1% formaldehyde (Sigma) at 25℃ for 20 minutes and quenched with 0.125 M Glycine for 5 minutes. After lysed with glass beads, chromatin pellet was sonicated by Bioruptor (Diagenode) to DNA fragment size about 200-500 bp in length, then immunoprecipitated with specific antibody in demand (Rfa1 and Rfa2 antibodies were gifts from Steven Brill lab). All ChIP DNA was enriched applying indicated antibody except TAP-tagged ChIP requires IgG beads (GE Healthcare) without further recognition by Protein G Sepharose (GE Healthcare). After extensive washing, chromatin was boiled with 10% Chelex 100 (Biorad) to reverse-crosslinking. The final ChIP DNA product was analyzed by Real-time PCR (CFX96; BioRad) with primers amplifying replication origins as well as its downstream regions. All primer sequences were listed in Appendix Table S2. Percentage of ChIP DNA relative to total input DNA was calculated. At least three independent biological repeats were performed and average results were calculated and presented, P values were determined using the unpaired Student t test using Prism software (GraphPad Software, Inc.). For Rfa1-TAP ChIP analysis in cell cycle progression, we performed non-parametric statistical analysis (single-tailed Wilcoxon test) of Rfa1-TAP signal at early S phase (30 min or 45 min) with Null Hypothesis H0: $level_{rtt105\Delta} >= level_{WT}$ by software R (v3.2.4). The results effectively rejected the Null Hypothesis (H0), and showed that in comparison with wild-type cells, the Rfa1-TAP signal was significantly reduced at replicating DNA during normal S phase in *rtt105*Δ mutant cells.

Fluorescence Microscopy

Haploid cells with indicated genotypes (GFP, mCherry tagging at C

terminus of certain chromosomal locus) were incubated in YPD or SCM synthetic drop-out media lacking key amino acid at 30℃. As for Galactose induction assay, cells were cultured in 2% Raffinose SCM liquid containing 0.002% glucose to support growth at first. After washing in ddH_2O, cells were resuspended in 2% Galactose SCM liquid and began induction. For Fluorescent Microscopy, all cells were harvested at OD_{600} no more than 0.5 during log phase. Pellets were washed in 1X PBS (pH 7.5) twice before mounted on microscope slides. For DAPI staining, cells were fixed in 70% ethanol for 2 mins, then treated with 1 μg/ml (final concentration) DAPI (Sigma) for 1-2 mins, washed with 1X PBS (pH 7.5) again before mounted on slide. All results were obtained using DeltaVision Personal DV System (Applied Precision) and Ultraview Vox Spinning Disk Confocal Microscopy (PerkinElmer) equipped with Velocity software (PerkinElmer). Image manipulation other than adjustments of brightness and contrast were not performed. Quantification and counting of microscopy data was present with at least 150 cells per experiment otherwise indicated in the figure legends by calculating the mean and SD of triplicate experiments. GFP and mCherry tagging plasmids (pKCG11 and pFA6a-yEmCherry-KIURA3) were kind gifts from Dr. Chao Tang (Peking University).

Bimolecular Fluorescence Complementation (BiFC)

The plasmid of pYFP-C1 is a gift from Dr. Yujie Sun. Cloning N terminal fragment of YFP (Vn173) to p423/Gal. Then insert sequence of *RTT105* to the N terminal of Vn173, linked with GGGGSGGGGS. Cloning C terminal of YFP (Vc155) to pRS315 and insert *KAP95* or *RFA1* to the N terminal of VC155, linked with GGGGGSGGGGS. Yeast strain Nup49-mCherry (LQY2151) was co-transformed with p423/Gal-Rtt105-Vn173 and pRS315-KAP95-Vc155 (or pRS315-Rfa1-Vc155). And cells are cultured in SCM-His-Leu medium with 2% raffinose. For BiFC, washing cells and transfer cells into medium with 2% Galactose, and induce 4 hours, followed by imaging. All the data is acquired on

Ultraview Vox Spinning Disk Confocal Microscopy (PerkinElmer) and processed by Velocity software (PerkinElmer).

Determining the dNTP levels

Yeast cultures were grown exponentially to a density of 0.5 to 0.7 × 10^7 cells/ml. For collecting asynchronous growing cells, ~5.6 × 10^8 cells (as determined by OD_{600}) were harvested by filtration through 25 mm White AAWP nitrocellulose filters (0.8 μm, Millipore). For G1 phase cells, asynchronous cultures at density of 0.5 x 10^7 cells/ml were treated with 5 μg/ml alpha factor (1000X) twice for 1.5 hour each to synchronize cells to G1 phase and were harvested as described above. Collected cells were further processed as described in(Jia et al, 2015). Briefly, NTPs and dNTPs were extracted in 700 μl ice-cold trichloroacetic acid-$MgCl_2$ solution [12% (wt/vol) trichloroacetic acid, 15 mM $MgCl_2$], followed by two rounds of neutralization by Freon-trioctylamine mixture [10 mL of Freon (1,1,2-trichloro-1,2,2-trifluoroethane); Sigma–Aldrich Sweden AB (>99%) and 2.8 mL of trioctylamine; Sigma–Aldrich Sweden AB (98%)]. 475 μL of the aqueous phase was pH-adjusted with 1 M ammonium carbonate (pH 8.9), loaded on boronate columns (Affi-Gel Boronate Gel; Bio-Rad), and eluted with a 50 mM ammonium carbonate (pH 8.9) and 15 mM $MgCl_2$ mixture to separate dNTPs from NTPs. The eluates containing dNTP only, were adjusted to pH 3.4 and analyzed by HPLC on a LaChrom Elite HPLC system (Hitachi) with a Partisphere SAX HPLC column (Hichrom). Nucleotides were isocratically eluted using 0.36 M ammonium phosphate buffer (pH 3.4, 2.5 % v/v acetonitrile). NTPs were directly analyzed by HPLC similar to dNTPs by using 47.5-μL aliquots of the aqueous phase adjusted to pH 3.4. Results from dNTP measurements were normalized to NTP levels of the cells.

Gross chromosome rearrangement (GCR) assay

GCR rate was determined by a quantitative assay for YAC telomere marker loss as previously described (Huang & Koshland, 2003). Briefly, yeast cells with

YACs (yWSS349 or yWSS349-5oriΔ) were streaked for single colonies on SCM-URA plates to select for the cell containing YAC telomere marker (URA3). The picked cells were resuspended in ddH_2O, diluted, and plated onto rich YPD plates to allow cells grow at 23°C. Colonies on the YPD plates were then replica-plated to both SCM-TRP and SCM-URA plates for growing at 23°C for 3-4 days. The growth of colonies was scored, and telomere marker loss rate was calculated using the number of cells with the YAC but lost of telomere marker (TRP+ URA-) to divide the number of cells with both YAC and telomere marker (TRP+ URA+).

Calculation of association constant (combine with EMSA)

The association constant (K_a) was calculated using Langmuir isotherm (Bastin-Shanower & Brill, 2001; Kim et al, 1994).

$$p = \frac{(kD) + (kR + 1) - \sqrt{((kD) + (kR) + 1)^2 - (4k^2DR)}}{2k}$$

Where p is the binding product concentration, k = association constant, D = total ssDNA concentration, R = total protein concentration. Simulation was performed by least-square method from the fit toolbox in MATLAB (R2015b) to get the association constant.

Supplemental references:

Bastin-Shanower SA, Brill SJ (2001) Functional analysis of the four DNA binding domains of Replication Protein A: the role of RPA2 in ssDNA binding. *The Journal of biological chemistry* **276:** 36446-36453

Binz SK, Dickson AM, Haring SJ, Wold MS (2006) Functional assays for replication protein A (RPA). *Methods in Enzymology* **409:** 11-38

Fan J, Pavletich NP (2012) Structure and conformational change of a replication protein A heterotrimer bound to ssDNA. *Genes & Development* **26:** 2337-2347

Huang D, Koshland D (2003) Chromosome integrity in Saccharomyces cerevisiae: the interplay of DNA replication initiation factors, elongation factors, and origins. *Genes & Development* **17:** 1741-1754

Jia S, Marjavaara L, Buckland R, Sharma S, Chabes A (2015) Determination of Deoxyribonucleoside Triphosphate Concentrations in Yeast Cells by Strong Anion-Exchange High-Performance Liquid

Chromatography Coupled with Ultraviolet Detection. In *DNA Replication: Methods and Protocols*, Vengrova S, Dalgaard J (eds), pp 113-121. New York, NY: Springer New York

Kim C, Paulus BF, Wold MS (1994) Interactions of human replication protein A with oligonucleotides. *Biochemistry* **33:** 14197-14206

Kim H-S, Brill SJ (2001) Rfc4 interacts with Rpa1 and is required for both DNA replication and DNA damage checkpoints in Saccharomyces cerevisiae. *Molecular and Cellular Biology* **21:** 3725-3737

Li Q, Zhou H, Wurtele H, Davies B, Horazdovsky B, Verreault A, Zhang Z (2008) Acetylation of histone H3 lysine 56 regulates replication-coupled nucleosome assembly. *Cell* **134:** 244-255

Nelson JD, Denisenko O, Bomsztyk K (2006) Protocol for the fast chromatin immunoprecipitation (ChIP) method. *Nature Protocols* **1:** 179-185

Park C-J, Lee J-H, Choi B-S (2005) Solution structure of the DNA-binding domain of RPA from Saccharomyces cerevisiae and its interaction with single-stranded DNA and SV40 T antigen. *Nucleic Acids Research* **33:** 4172-4181

Puig O, Caspary F, Rigaut G, Rutz B, Bouveret E, Bragado-Nilsson E, Wilm M, Séraphin B (2001) The tandem affinity purification (TAP) method: a general procedure of protein complex purification. *Methods* **24:** 218-229

Thomas BJ, Rothstein R (1989) Elevated recombination rates in transcriptionally active DNA. *Cell* **56:** 619-630

Viggiani CJ, Aparicio OM (2006) New vectors for simplified construction of BrdU-Incorporating strains of Saccharomyces cerevisiae. *Yeast* **23:** 1045-1051

Zou L, Elledge SJ (2003) Sensing DNA Damage Through ATRIP Recognition of RPA-ssDNA Complexes. *Science* **300:** 1542